Nanoscale Res Lett (2009) 4:834–838
DOI 10.1007/s11671-009-9325-7

NANO EXPRESS

Facile Synthesis of Ternary Boron Carbonitride Nanotubes

Lijie Luo · Libin Mo · Zhangfa Tong · Yongjun Chen

Received: 1 March 2009 / Accepted: 14 April 2009 / Published online: 5 May 2009
© to the authors 2009

Abstract In this study, a novel and facile approach for the synthesis of ternary boron carbonitride (B–C–N) nanotubes was reported. Growth occurred by heating simple starting materials of boron powder, zinc oxide powder, and ethanol absolute at 1150 °C under a mixture gas flow of nitrogen and hydrogen. As substrate, commercial stainless steel foil with a typical thickness of 0.05 mm played an additional role of catalyst during the growth of nanotubes. The nanotubes were characterized by SEM, TEM, EDX, and EELS. The results indicate that the synthesized B–C–N nanotubes exhibit a bamboo-like morphology and B, C, and N elements are homogeneously distributed in the nanotubes. A catalyzed vapor–liquid–solid (VLS) mechanism was proposed for the growth of the nanotubes.

Keywords B–C–N nanotubes · Synthesis · Stainless steel foil · Characterization · VLS model

Introduction

Ternary boron carbonitride (B–C–N) nanotubes have recently attracted much attention because of their excellent mechanical properties, electrical properties, and anti-oxidant capacities [1, 2]. In addition, theoretical studies have revealed that the band gaps of B–C–N nanotubes can be tailored over a wide range by simply varying the chemical composition rather than by geometrical structure [3–7], which is superior to their carbon and boron nitride (BN) counterparts. This gives B–C–N nanotubes potential for use in electronics, electrical conductors, high temperature lubricants, and novel composites [8]. Compared with the very extensive study about carbon and BN nanotubes, however, very little work was reported about B–C–N nanotubes. Since the discovery of B–C–N nanotubes in 1994 [9], several methods have been devoted to the synthesis of B–C–N nanotubes, such as arc-discharge [10], laser ablation [11], chemical vapor deposition (CVD) [12, 13], template route, and pyrolysis techniques [14, 15]. Particularly, single-walled B–C–N nanotubes have been recently synthesized by Wang et al. [16] via a bias-assisted hot-filament method. However, most of them usually used risky reagents such as diborane (B_2H_2)/ammonia (NH_3), or produced nanotubes with low purity and high-cost and encountered the phase separation problem of BN and C. Thus, it is of great significance to explore novel and simple routes to prepare B–C–N nanotubes with uniform distribution of component B, C, and N elements. The current work reports a relatively safe and effective approach for growing high-purity B–C–N nanotubes directly on commercial stainless steel foil, by using simple raw materials of boron, zinc oxide (ZnO), and ethanol absolute. The reaction of boron and ZnO at high temperature produces boron oxide vapor that is the source of B, while ethanol absolute and nitrogen provide the source of C and N, respectively. It is interesting that the stainless steel foil is not only the support substrate but also the catalyst for the growth of the nanotubes. The obtained nanotubes have an average diameter of about 90 nm and the B, C, and N elements are found to be homogeneously distributed in the nanotubes. The growth mechanism of the nanotubes is also investigated in this study. To the best of our knowledge, it is the first time to report the synthesis of

L. Luo · L. Mo · Z. Tong · Y. Chen (✉)
School of Chemistry and Chemical Engineering, Guangxi University, Nanning 530004, China
e-mail: yongchen@gxu.edu.cn

ternary B–C–N nanotubes via such a relatively simple route.

Experimental Methods

The growth of nanotubes was carried out in a conventional tube furnace. An alumina boat loaded with about 1.0 g mixture of hexagonal ZnO and amorphous B powder (with a ZnO:B molar ratio of 1.5:1) was inserted into a quartz tube and placed at the center of the furnace. Commercial stainless steel-304 foil with a thickness of 0.05 mm was inserted into the quartz tube as the substrate. Prior to heating, the chamber was flushed with high-purity N_2 flow to eliminate the residual air. Then the furnace was heated to 1150 °C under a mixture gas flow of N_2 (60 mL min^{-1}) and H_2 (40 mL min^{-1}). Ethanol absolute (AR grade) was introduced into the chamber when the furnace temperature reached at 1150 °C, which was carried by another N_2 flow with a rate of 20 mL min^{-1}. The furnace was maintained at 1150 °C for 90 min. Finally, the furnace was cooled naturally to ambient temperature under the protection of N_2 flow. After taken from the furnace, the stainless steel substrate was found to be covered with white–gray deposit in the temperature range of 1000–1100 °C. The product was characterized by field-emission scanning electron microscopy (FE-SEM, Hitachi S5500), high-resolution transmission microscopy (HRTEM, JEM-2010F), X-ray energy dispersive spectrometer (EDS), and electron energy loss spectroscopy (EELS), respectively.

Results and Discussion

Figure 1 shows the SEM images of the product grown on the surface of stainless steel substrate. Low-magnification image (Fig. 1a) indicates a high production of one-dimensional (1D) nanostructures was synthesized. The inset in Fig. 1a is a high-magnification cross-sectional image of some 1D nanostructures, illustrating the hollow structure of the product. Figure 1b clearly reveals that the nanotubes are shaped in bamboo consisting of a number of compartments. The surfaces of the nanotubes are very clean and no impurities can be observed, which indicates the high purity of the nanotubes. The diameters of the nanotubes are approximately 60–120 nm, with an average value of about 90 nm. Furthermore, it can also be found that nanoparticles are attached at the ends of nanotubes, which could be regarded as a typical symbol of vapor–liquid–solid (VLS) growth model. Figure 1c and d are the secondary electron and back scattering electron (BSE) images of the same area of the product. It can be seen that the attached particles (bright particles) are distinguished clearly in the BSE image, which further confirms the VLS growth mechanism of the nanotubes.

The TEM images of the product are shown in Fig. 2. Similar to SEM observation, the bamboo structure of the nanotubes with clean surface and uniform diameter along the nanotube length can be clearly seen (Fig. 2a). The inset in Fig. 2a is the EDX result, which shows the dominating peaks of B, C, and N with a low level of O, Cu, and Si. The existence of Cu peak should be caused by the copper TEM

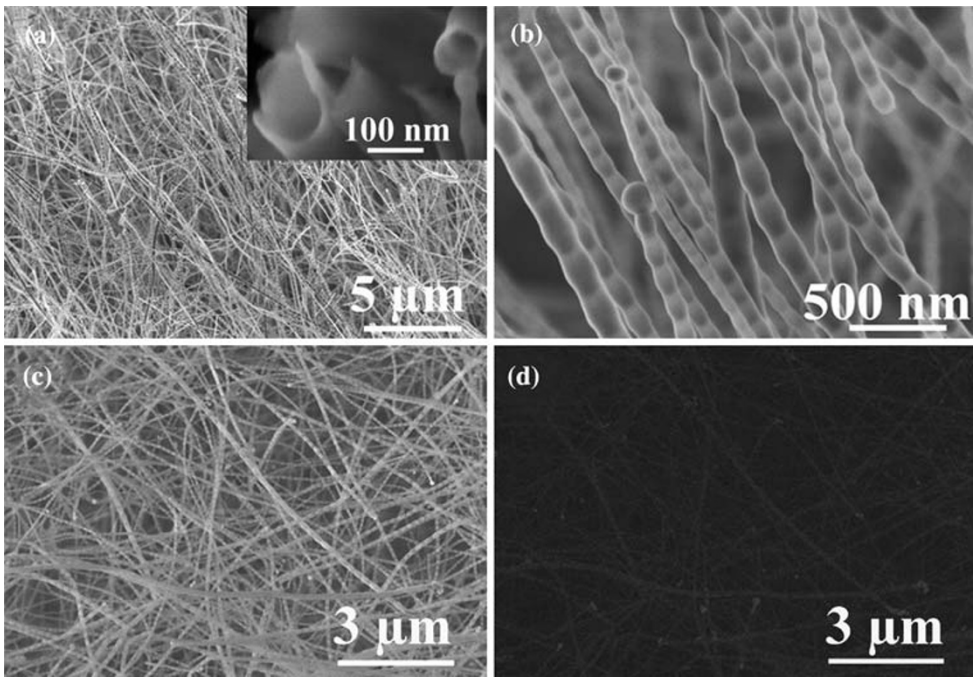

Fig. 1 **a** Low-magnification SEM image of the product, showing the large quantity of the 1D product grown on the stainless steel substrate. The inset is the high-magnification cross-sectional image of some nanotubes, illustrating the hollow structure. **b** High-magnification image of **a**, indicating the bamboo-like structure and high purity of the nanotubes. **c** and **d** The secondary electron and back scattering electronic (BSE) SEM images of the same area of the product

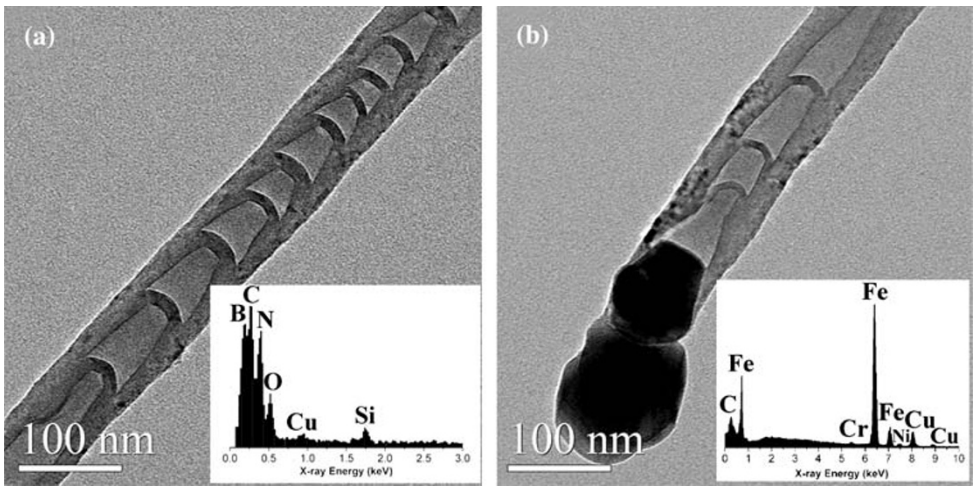

Fig. 2 **a** TEM image of a nanotube. The inset is the EDX spectrum of the nanotube. **b** TEM image shows a catalyst particle attached at the end of a nanotube. The inset is the EDX spectrum of the particle

grid, while the Si peak might come from the stainless steel substrate. The O peak can be ascribed to the slight surface oxidation of the nanotube. Furthermore, quantitative analysis gives the B:C:N atomic ratio of about 0.45:0.31:0.24. Therefore, it can be roughly concluded that the synthesized nanotubes are B–C–N nanotubes. In Figure 2b, a particle attached at the end of the nanotube is clearly seen, which is also consistent with SEM observation. The EDX spectrum indicates that the particle is mainly composed of Fe with a small amount of Ni, Cr, Cu, and C (inset in Fig. 2b). As mentioned above, the Cu and C peaks should come from the carbon film-coated copper grid. While the existence of Fe, Ni, and Cr in the particle should originate from the stainless steel substrate. Hence, we believe that the stainless steel substrate play a catalyst role during the VLS growth of the nanotubes.

Figure 3a shows the HRTEM image of the edge part of the nanotube wall. It can be seen that the lattice fringes are

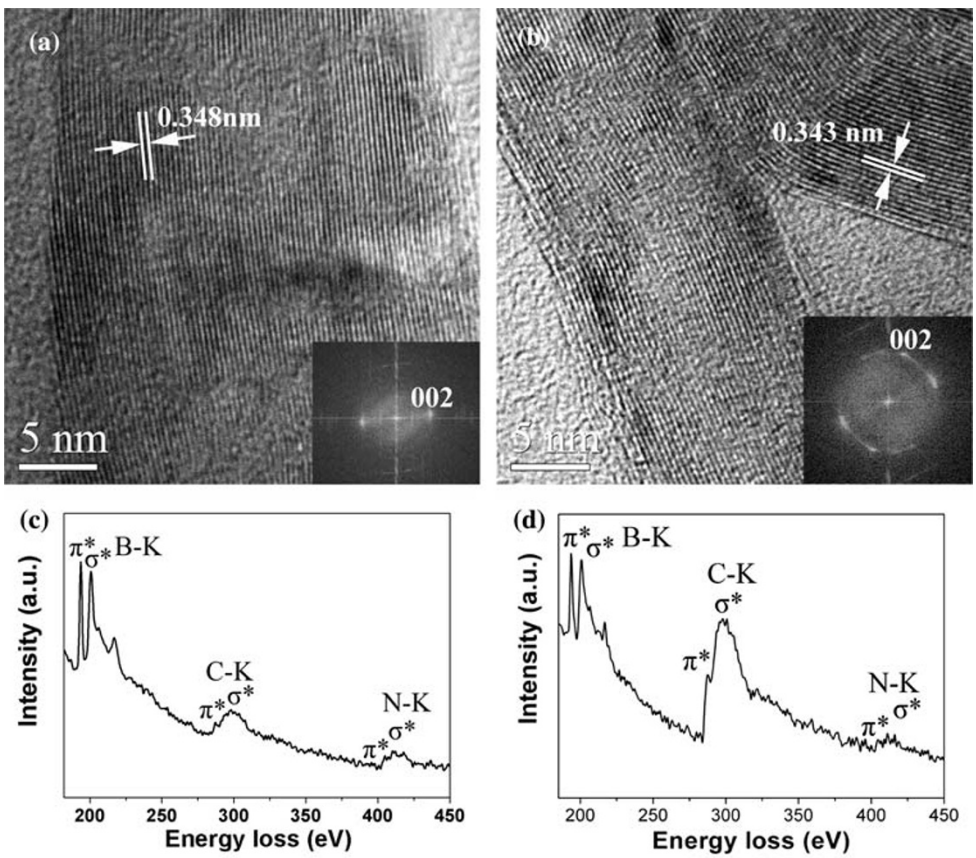

Fig. 3 **a** HRTEM image of nanotube wall and the corresponding FFT ED pattern (inset). **b** HRTEM image of a joint between the wall and compartment and the corresponding FFT ED pattern (inset). **c** and **d** EELS spectra taken from the nanotube wall and the compartment, respectively, revealing the dominating composition of B, C, and N elements in the wall and compartment

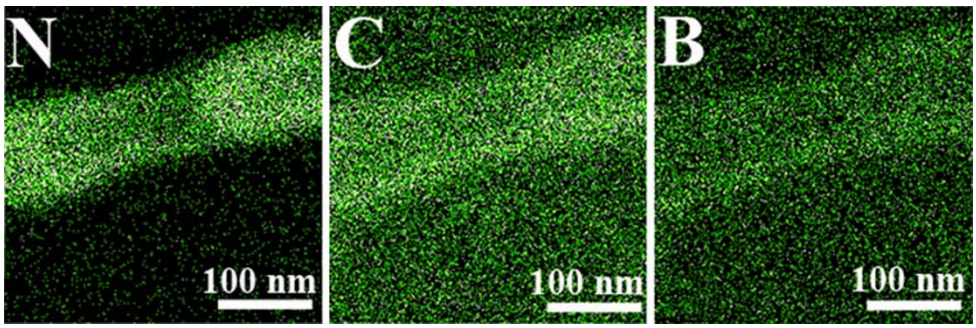

Fig. 4 Elemental maps of a nanotube, implying the uniform distribution of the B, C, and N species in the nanotube

well-defined, which suggests that the nanotube wall has a high degree of crystalline perfection. The interlayer spacing is approximately 0.348 nm, corresponding to the (002) plane of hexagonal system of B–C–N crystal (JCPDS No. 35-1292). The spots in the fast Fourier-transformed ED (FFT ED) pattern can be indexed as the (002) basal planes of the B–C–N layers (inset in Fig. 3a). Figure 3b is the HRTEM image of the joint, showing the tight connection between nanotube wall and compartment. The compartment is also well-crystallized with the identical lattice spacing of about 0.343 nm, which also corresponds to the (002) plane of B–C–N crystal. The FFT ED pattern (inset in Fig. 3b) is also indexed as the (002) planes of B–C–N crystal. Figure 3c shows a representative EELS spectrum taken from a segment of the nanotube wall, which demonstrates that the distinct absorption peaks of B, C, and N characteristic K-edges at 188, 201, and 401 eV, respectively. The result further proves the nanotube composition of B–C–N. The K-edge signals show a discernible π^* peak, as well as an σ^* band, indicating that the B, C, and N atoms are in the sp^2-hybridized state. The EELS spectrum of the compartment shown in Fig. 3d also indicates the distinct absorption features of K-edges of B, C, and N atoms. Furthermore, the elemental maps reveal that B, C, and N elements are homogeneously distributed in the nanotube (Fig. 4). Therefore, it can be concluded that the product is composed of ternary compound B–C–N nanotubes.

As described above, a simple approach to synthesize B–C–N nanotubes was proposed by involving an additional role of catalyst of the stainless steel substrate. And based on the above results, VLS model is believed to be responsible for the growth of the current nanotubes. Similar to the literatures reported about BN nanotubes and nanowires [17–19], Fig. 5 illustrates schematically the suggested growth process of the B–C–N nanotubes. Firstly, the reaction of B and ZnO generates Zn and boron oxide (B_2O_2) vapor at high temperature (1150 °C). Meanwhile, the surface of the stainless steel may partially melt at this temperature assisted by the erosion of N_2 and H_2. And thus liquid alloy droplets with main composition of Fe–Cr–Ni are formed on the surface, as are verified by the EDX result. Then the liquid droplets adsorb the growth species

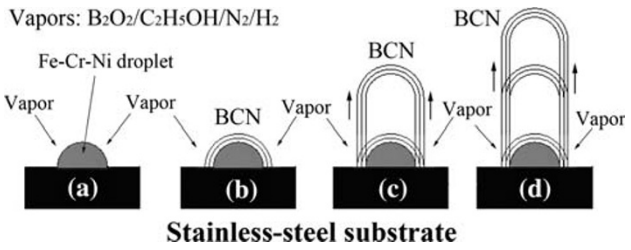

Fig. 5 The schematic diagram of the B–C–N nanotube growth on the stainless steel substrate

from the surrounding vapors of B_2O_2, C_2H_5OH, N_2, and H_2 (Fig. 5a). The involving species of B and C could lead to the further decrease of the melting temperature of stainless steel and promotes the formation of liquid droplets. The reactions among these vapors produce B/C/N atoms, which diffuse through Fe–Cr–Ni alloy droplets. When the concentrations of species are greater than the saturation threshold, B–C–N crystals begin to precipitate and initially form the cap on the liquid droplets, as is shown in Fig. 5b. With the continuous supply of B/C/N atoms, the cap will be lift from the droplet due to the stress under the curvature and then the hollow tip forms. At the same time, due to the diffusion of B/C/N atoms through the surface and bulk, the B–C–N sheets also grow and form the nanotube wall. When the nanotube wall grows, the B/C/N atoms also precipitate inside the nanotube and result in the formation of compartment layer. The compartment layers connect with the wall and grow together for a period, and finally depart from the droplet due to the stress accumulated under the curved compartment layers (Fig. 5c). As the joint between compartment and wall forms periodically, the bamboo-like structure is formed (Fig. 5d). Moreover, the flowing character of B_2O_2, C_2H_5OH, N_2, and H_2 vapors could lower their partial pressures in the chamber, which is also favorable for the formation of 1D nanotubes. It should be noted that the produced Zn vapor is transported by the carrier gas to a much lower temperature zone (below the melting point of Zn), where it deposits on the substrate in the form of Zn products [20]. Therefore, the synthesized B–C–N nanotubes are not contaminated by Zn products. In addition, it is found that the hydrogen in the mixture gas is

essential for the growth of B–C–N nanotubes. If only pure N_2 flow is introduced, no B–C–N nanotubes can be obtained, adding weight to the proposed mechanism and suggesting that hydrogen plays an important role during the growth of the B–C–N nanotubes.

Conclusion

In summary, a simple but efficient route to synthesize B–C–N nanotubes directly onto commercial stainless steel foil is demonstrated by using raw materials of boron powder, zinc oxide powder, and ethanol absolute. The nanotubes are pure with bamboo-like morphology and an average diameter of about 90 nm. During the formation process, the stainless steel foil plays a catalyst role additionally besides the substrate role for the B–C–N nanotube growth. A VLS process is proposed to be responsible for the growth of the B–C–N nanotubes.

Acknowledgments The authors acknowledge financial support from the National Natural Science Foundation of China (NSFC, Grant No. 50862001), Ministry of Education of China (MOE, Grant No. 208106), Tsinghua University State Key Laboratory of New Ceramics & Fine Processing and Guangxi University (Grant No. DD040042).

References

1. A.Y. Liu, R.M. Wentzcovitch, M.L. Cohen, Phys. Rev. B **39**, 1760 (1989). doi:10.1103/PhysRevB.39.1760
2. P. Dorozhkin, D. Golberg, Y. Bando, Z.C. Dong, Appl. Phys. Lett. **81**, 1083 (2002). doi:10.1063/1.1497194
3. S.Y. Kim, J. Park, H.C. Choi, J.P. Ahn, J.Q. Hou, H.S. Kang, J. Am. Chem. Soc. **129**, 1705 (2007). doi:10.1021/ja067592r
4. L. Liao, K.H. Liu, W.L. Wang, X.D. Bai, E.G. Wang, Y.L. Liu, J.C. Li, C. Liu, J. Am. Chem. Soc. **129**, 9562 (2007). doi:10.1021/ja072861e
5. Y. Miyamoto, A. Rubio, M.L. Cohen, S.G. Louie, Phys. Rev. B **50**, 4976 (1994). doi:10.1103/PhysRevB.50.4976
6. A.M. Enyashin, Y.N. Makurin, A.L. Ivanovskii, Carbon **42**, 2081 (2004). doi:10.1016/j.carbon.2004.04.014
7. X. Blase, J.C. Charlier, A.D. Vita, R. Car, Appl. Phys. Lett. **70**, 197 (1997). doi:10.1063/1.118354
8. M. Kawaguchi, Adv. Mater. **9**, 8 (1997). doi:10.1002/adma.19970090805
9. O. Stephan, P.M. Ajayan, C. Colliex, P. Redlich, J.M. Lambert, P. Bernier, P. Lefin, Science **266**, 1683 (1994). doi:10.1126/science.266.5191.1683
10. K. Suenaga, C. Colliex, N. Demoncy, A. Loiseau, H. Pascard, F. Willaime, Science **278**, 653 (1997). doi:10.1126/science.278.5338.653
11. P. Redlich, J. Loeffler, P.M. Ajayan, J. Bill, F. Aldinger, M. Rühle, Chem. Phys. Lett. **260**, 465 (1996). doi:10.1016/0009-2614(96)00817-2
12. X.D. Bai, J.D. Guo, J. Yu, E.G. Wang, J. Yuan, W.Z. Zhou, Appl. Phys. Lett. **76**, 2624 (2000). doi:10.1063/1.126429
13. L.W. Yin, Y. Bando, D. Golberg, A. Gloter, M.S. Li, X. Yuan, T. Sekiguchi, J. Am. Chem. Soc. **127**, 16354 (2005). doi:10.1021/ja054887g
14. M. Terrones, D. Golberg, N. Grobert, T. Seeger, M. Reyes-Reyes, M. Mayne, R. Kamalakaran, P. Dorozhkin, Z.C. Dong, H. Terrones, M. Rühle, Y. Bando, Adv. Mater. **15**, 1899 (2003). doi:10.1002/adma.200305473
15. S. Rahul, B.C. Satishkumar, A. Govindaraj, K.R. Harikumar, R. Gargi, J.P. Zhang, A.K. Cheetham, C.N.R. Rao, Chem. Phys. Lett. **287**, 671 (1998). doi:10.1016/S0009-2614(98)00220-6
16. W.L. Wang, X.D. Bai, K.H. Liu, Z. Xu, D. Golberg, Y. Bando, E.G. Wang, J. Am. Chem. Soc. **128**, 6530 (2006). doi:10.1021/ja0606733
17. C.C. Tang, Y. Bando, T. Sato, K. Kurashima, Chem. Commun. (Camb) **12**, 1290 (2002). doi:10.1039/b202177c
18. N. Kio, T. Oku, M. Inoue, K. Suganuma, J. Mater. Sci. **43**, 2955 (2008). doi:10.1007/s10853-007-1750-3
19. Y.J. Chen, B. Chi, D.C. Mahon, Y. Chen, Nanotechnology **17**, 2942 (2006). doi:10.1088/0957-4484/17/12/020
20. Y.J. Chen, B. Chi, H.Z. Zhang, H. Chen, Y. Chen, Mater. Lett. **61**, 144 (2007). doi:10.1016/j.matlet.2006.04.044